Novel Space-Time Helicopter Flight Display

Edward Bachelder

San Jose State University
U.S. Army Aviation Development Directorate
Moffett Field, California 94035

Abstract. A helicopter's final approach and landing are critical phases of the flight that are highly susceptible to spatial disorientation when external visual cues become degraded. Current helicopter visual landing aid systems display instantaneous flight path tracking error which the pilot attempts to null in a compensatory fashion. This paper presents theoretical and empirical support for performance enhancement when providing pilots a near-future preview of the states they intend to track, rather than just a compensatory display of the tracking error. A novel space-time format is proposed for displaying: 1) Previewed guidance information; 2) Projected (predicted) state relative to the guidance preview; and 3) Current state relative to current guidance and terminal objectives. A key objective of the display is to allow the pilot to perceive and control each axis of translation as part of an integrated pattern, thus distributing attention equitably. A prediction algorithm was developed from the perspective of manual control theory, specifically, employing McRuer's human crossover model. A preliminary simulation experiment was conducted to investigate the efficacy of the new display format and the effects of predictor design using previewed guidance. Results showed that pilots rapidly adapted to the display, and demonstrated high precision and accuracy when flying an aggressive approach-to-land maneuver.

1 INTRODUCTION

Humans naturally navigate through their physical environment using the native display provided by their eye-point. Highly-skilled self-motion tasks such as gymnastics and car racing require precision both in timing and amplitude of execution, motion that appears to be governed by time-to-collision (tau theory) [1], or a combination of time-to-collision and precognitive (open-loop) behavior. These demanding tasks tend to be very repetitive and are supported by refined sensing and motor skills. If one or more of these three conditions is absent (i.e. the task setting becomes unfamiliar, visibility is reduced, fatigue impairs response), the risk of improper execution increases. But the cornerstone is perception, whether of states at the start of an open-loop maneuver, or continuous perception of time-to-collision intuited from state derivative comparison.

A complicating aspect of human visual perception is that transverse motion cues (left/right, up/down relative to the line-of-sight) are lamellar and fundamentally different from the radial cues produced by motion in the depth axis (fore/aft). In reference In a study conducted in 2000 [2], Bachelder investigated the effect of translation cue effect on manual control. In this study a helicopter simulation experiment employed a number of unique techniques designed to create an environment where differences in performance between axes would be due primarily to visual perception and control strategy differences. In the experiment depth cues were artificially magnified so that the angular sensitivity of motion cues were equal in all three axes of translation (fore/aft, left/right, up/down). It should be noted that without artificial magnification, sensitivity to depth motion is approximately 20 times less than transverse motion sensitivity [2] (when the cues are observed within foveal vision, approximately +/- 3 degrees). Each axis of vehicle translation was governed by the same dynamics, and the controls were all spring-centering. During single-axis control (where one axis was active and the other two disabled), stability margins and tracking performance were roughly the same for all three axes. However, simultaneous tracking in all three axes yielded

statistically significant interaction effects and differences between axes. By varying motion cue sensitivity in one axis and observing performance change in the others, it was concluded that the depth axis receives more attentional resources than the others, i.e. motion in depth is more compelling. Performance during multi-axis tracking was best in the lateral axis.

There are numerous displays used for spatial aiding in aviation, examples include: vertical situation and navigation (Fig. 1a), Instrument Landing System, moving map, electronic approach plate, and optical landing systems. The Head-up-Display (HUD, Fig. 1b) allows the flight path vector and other world-conformal symbology to be overlaid on the actual out-the-window (OTW) scene. More recently, synthetic vision (SV) provides pilots with a computer-generated representation of the OTW scene. Tunnel-in-the-sky [3] symbology can be used with SV to provide pilots current and future guidance cueing (Fig. 2).

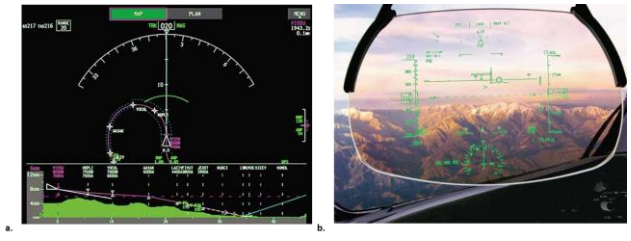

Fig. 1. Boeing 787 displays: a) Navigation and vertical situation display; b) HUD [4].

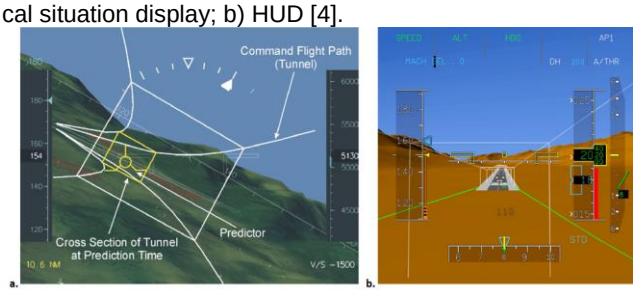

Fig. 2. Tunnel-in-sky cueing: a) Curved approach [5]; b) Landing guidance [6].

Specific to helicopters, displays such as the Apache Integrated Helmet and Display Sighting System (IHADSS) depict the landing area relative to current position, as well as guidance for acquiring the landing pad position.

Visual aids that employ multiple planes to represent space (such as horizontal and vertical planes shown in Fig. 1a) generally require the operator to dedicate attention to one plane at the expense of the other. When decision/action events between planes are sufficiently separated in time, this segmented approach can provide acceptable performance and pilot workload. However, when events in both planes coalesce, division of attention can produce high workload and increase the risk for error.

3D displays allow guidance to be embedded in the scene that the pilot captures maneuvering throughout that scene, but there are challenges with this approach. Guidance cues closest to ownship's position will appear larger than distant cues, and near and far cues often overlap. When they do, cascading cues (boxes, for instance) can obscure prospective guidance and diminish the advantage of preview, while interfering with perception of the proximal guidance cues. Furthermore, clutter due to cue coalescence along the line-of-flight can reduce visibility of, and create competition with, physical goals such as the runway during approach-to-land. Commanded speed changes in 3D guidance can be implied via cue density, where closer spacing denotes a slower speed, but this only imparts a general sense of future speed.

Fig. 3 presents the same trajectory using distance and time as the independent variables, respectively. In Fig. 3a time progression is denoted by dots shown at three-second intervals. Much of the trajectory is a constant flight path angle, and the sense for how altitude changes in time is difficult to perceive, especially near the maneuver's termination. However, when viewing altitude as a function of time in Fig. 3b, the temporal nuances of the trajectory are evident.

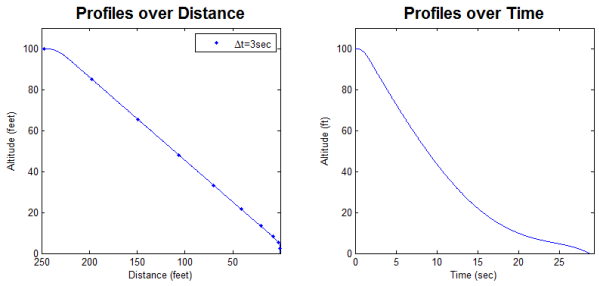

Fig. 3. Comparison of the same trajectory using a) distance; and b) time as the independent variable.

A workload-intensive maneuver such as landing requires precise, subtle control of both speed and altitude, and employing temporal inference via spatial cueing (i.e. inferring speed from cue spacing) may not offer significant assistance. Reference [6] reports that while 3D predictive guidance during landings improved the timing of flare initiation, actual execution of the flare was not enhanced by the predictive guidance. It is an unfortunate irony that augmenting a synthetic scene in the direction that one must look - along the line-of-motion – is such a difficult challenge.

During day (unrestricted visibility) flight, skilled helicopter pilots can perform aggressive and intricate approach-to-land maneuvers with relative ease. When flying in degraded or zero-visibility

conditions, the complexity of a trajectory is often dictated by the workload and performance associated with a particular display. Key metrics for evaluating a landing display should include: performance repeatability, robustness to external disturbance, graceful degradation as task difficulty increases, and robustness to lapses of attention, in addition to pilot workload and opinion.

2 DISPLAY DESIGN

Initially conceived at the U.S. Army Aviation Development Directorate as a 4D (time + 3D space) tool to evaluate candidate landing trajectories, the Aircraft Guidance Visualization Application (AGVA) was subsequently recognized as a potential platform for testing concepts which could be integrated with current and future landing displays. Developed in MATLAB, AGVA incorporates a Simulink model that receives inputs from a USB joystick/throttle gaming device plugged into a PC, providing the option for either automatic or pilot guidance-following. A powerful feature of the simulation is that the graphics are driven and rendered in real time thus allowing pilot-in-loop operation, a capability made possible through code optimization. AGVA also establishes the feasibility for portable rapid prototyping and testing of guidance-related flight symbology using a PC, laptop, or tablet.

2.1 Prediction and Preview

AGVA incorporates two complementary mechanisms that can improve performance and reduce pilot workload: guidance preview and state prediction. In his watershed work on human pilot behavior [7], McRuer proposed the Dual Channel model to represent how an operator blends a) previewed information of the reference signal being tracked with b) error between the reference and the system output. Fig. 4 shows the McRuer Dual Channel model modified to include time-projected feedforward, prediction feedback, and external disturbance. A time advance element operates on the guidance to generate the time projection T_{PR} which is used by the predictor H_{PR}, and the projected reference is then compared with the predicted system output. Y_r is the element representing the pilot's transfer function that operates on the previewed reference signal, and Y_e is the pilot compensatory element that operates on the error *e*. A disturbance *d* is added to the aircraft (G_c) output, with the predictor H_{PR} operating on the result.

Equation 1 gives the error-to-reference transfer function. If the disturbance d is zero, Equation 2 shows that the error *e* is driven to zero when Y_r becomes the inverse of the aircraft-predictor suite.

$$\frac{e(s)}{r(s)} = \frac{e^{sT_{PR}}(1 - Y_r H_{PR} G_c)}{(1 + Y_e H_{PR} G_c)} + \frac{[d(s)/r(s)]H_{PR}}{(1 + Y_e H_{PR} G_c)} \quad (1)$$

$$\text{if } Y_r \approx (H_{PR} G_c)^{-1} \text{ and } d(s) \approx 0 \Rightarrow e(s) \approx 0 \quad (2)$$

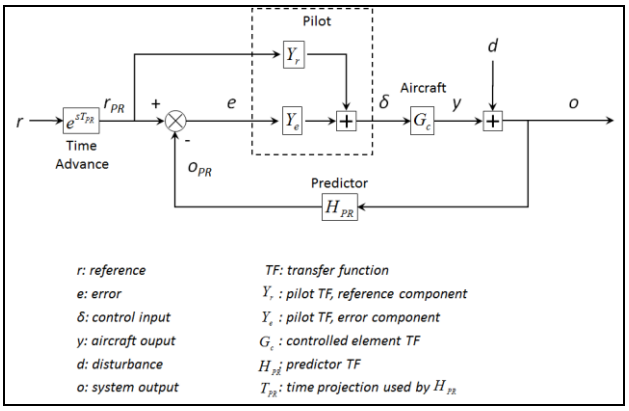

Fig. 4. Dual Channel model [8] modified to include prediction feedback and external disturbance.

However, since the pilot's actual transfer function corresponding to Y_r will vary over time and deviate from $(H_{PR}G_c)^{-1}$, and as disturbances (i.e. from wind) will impinge on the aircraft, the resulting error *e* must also be controlled by Y_e as shown in Fig. 4.

To examine system response to disturbance, the reference signal in Fig. 4 has been set to zero so that tracking becomes a regulation task as shown in Fig. 5. In this task the objective is to negate the disturbance *d*, hence the negative sign on *d*.

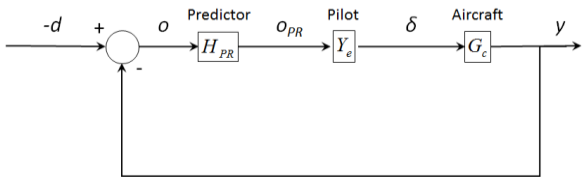

Fig. 5. Dual-Channel model from Fig. 4 reduced to compensatory control for regulation task (reference signal = 0).

McRuer established that compensatory control is easiest for a pilot when he/she can operate as a pure gain, which occurs when the controlled element G_c behaves approximately as a pure integrator K/s in the region of the gain crossover frequency ω_c. Later research showed this rule also applies to the display-vehicle suite. Since the predictor H_{PR} generates the display dynamics that the pilot responds to, the appropriate design for H_{PR} in the region of ω_c would be (Equation 3):

(3) $$H_{PR}(j\omega_c)G_c(j\omega_c) \approx \frac{K}{s} \Rightarrow Y_e \approx const$$

Equation 4 follows from Equation 2,

(4) $$Y_r \approx (H_{PR}G_c)^{-1} \approx \frac{s}{K}.$$

Generating pure lead of Equation 2 in response to the previewed guidance is relatively easy for a skilled pilot. One challenge associated with this approach can be preserving the temporal meaning of H_{PR}'s output so that it can be used with the time-referenced guidance. Of course, if the task is station-keeping, the guidance trajectory is zero over all time so that H_{PR}'s output does not need to correlate with time. But this is a special case, and the objective of AGVA is to address time-varying guidance in general.

The above analysis establishes that H_{PR} has the potential to optimize pilot performance when a previewed reference signal is being tracked in the presence of disturbance. A more detailed discussion of H_{PR} design considerations will be given later.

While most guidance displays are spatially-referenced, the motivations for making AGVA time-referenced were: 1) Preview of near-future guidance is interpreted with more ease when the pilot does not have to infer time by mentally integrating current and future speed; 2) Prediction cueing is projected along the guidance a consistent distance out (speed-invariant), allowing precise trajectory anticipation; 3) Since vehicle dynamics are significantly different for the three axes of translation, optimal prediction times for each axis will likely be different as well. A unique prediction time can be assigned to an axis of translation when there is a unique time axis dedicated to it. This is not possible in a spatially-referenced display; 4) Cueing curvature provides explicit and valuable information about the guidance and prediction derivatives (velocity, acceleration, even jerk); 5) Spatial resolution for each axis of translation is independent of the other, allowing state resolution to be a function of its rate of change, thus enhancing the utility of preview.

2.2 Display Description

AGVA displays key states associated with each axis of translation (position relative to landing zone, error from guidance, and rate of motion), as well as position, rate, and acceleration of future guidance. The altitude guidance is presented on the left side of the display (controlled by the left hand with the collective), and the lateral and longitudinal guidance are presented in the center and right, respectively (controlled by the right hand with the cyclic). Thus the spatial motion of the three axes is aligned with the reference frames that Army pilots are accustomed to flying (top-down view for cyclic control, profile view for collective control). As earlier noted, human sensitivity to transverse motion is greater than to depth motion, thus by representing 3D space on the transverse plane AGVA maximizes motion sensitivity and spatial resolution. Fig. 6a annotates most of the graphical features of AGVA. Three prediction segments, one for each axis of translation (altitude, distance-to-land, and cross-distance), are colored magenta, originating at display center and terminating at the predicted position. The three guidance trajectories originate from the center of the display. Ownship's current error from the guidance is denoted along each translation axis by a grey bar that originates from the axis' center to a magenta pointer. The time scale assigned to altitude is shown on the lower left of the display (horizontally aligned), the time axis assigned to distance on the lower right (horizontally aligned), and the time axis assigned to cross-distance is on the upper right (vertically aligned). Since the cross-distance time axis also overlaps with the distance (and altitude) axis, it is suppressed from view.

For ease of exposition, the AGVA prediction method employed in Fig. 6 simply integrates the instantaneous velocity over a fixed projection time (2 seconds in this example). The angle formed by the predictor's time axis and the prediction segment controls the segment's slope, which is the instantaneous velocity. Fig. 6b shows the velocity angles associated with each translation axis. A speed reference bar is placed at the end of a prediction segment - the point of intersection represents the current speed, at which location the value of the current speed is displayed. The base of the speed bar is placed flush with current position (i.e. the origin of the prediction segment), so that when speed approaches zero the prediction segment will lie parallel to its time axis. The end of the speed bar displays an upper reference value (which can be a not-to- exceed operating limit). The speed scale is nonlinear in order to maintain the reference bar in view. The distance axis scale is a function of forward speed, so that preview of the distance guidance will be visible over most of the time scale. The scales of altitude and cross-distance axes were fixed for the examples presented, since their speeds did not vary as much as the forward speed. However, if a trajectory required sufficiently large speed variation for any given axis, the resolution could be speed-dependent. Although providing less resolution at higher rates, this method is consistent with human perception (Weber's Law), according to which subjective sensation is proportional to the loga-

rithm of the stimulus intensity. In the present case, the faster the rate, the less precise the sense of distance traversed.

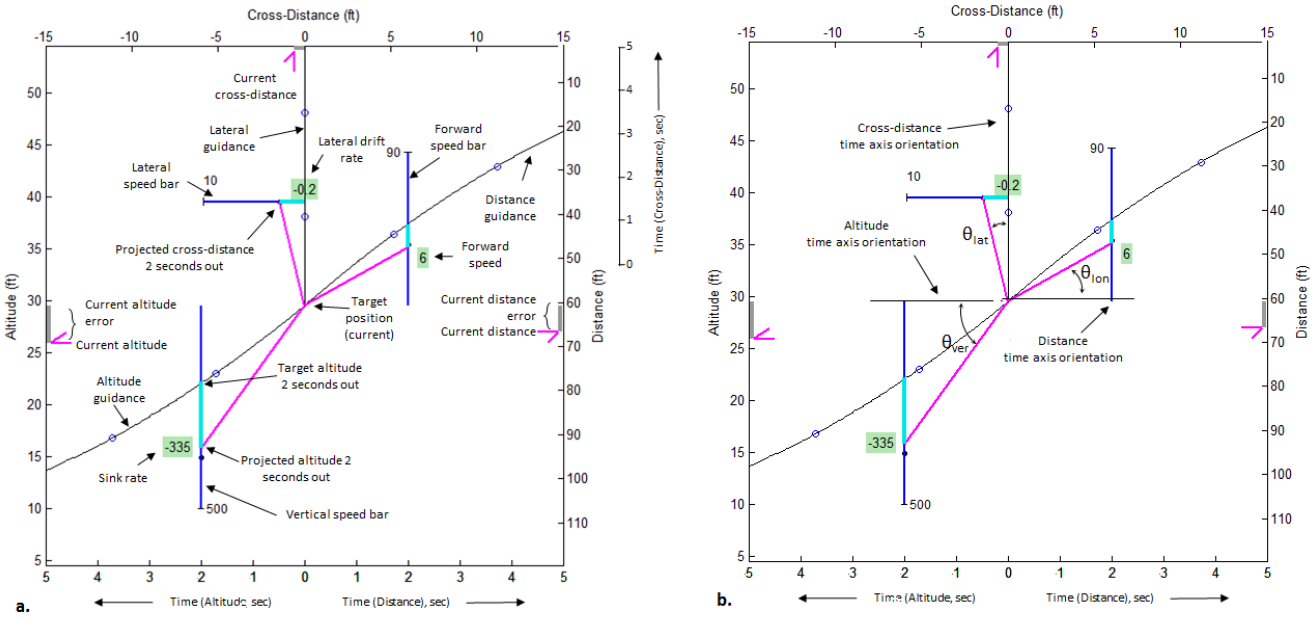

Fig. 6. Annotated AGVA display.

The tracking strategy when operating AGVA is to place the endpoint of each magenta prediction segment onto its axis' future guidance, which will result in closure of ownship's positional error along that axis. The distance between the future guidance and predicted position is highlighted in cyan, so that when the predictor overlays the guidance cyan is no longer visible. A zero-velocity end-state for any axis will result in the prediction segment lying flush with that axis at touchdown. If the terminal speed guidance is 0/0/0 for all axes, the pattern at the maneuver's finish would be an inverted 'T'. An axis' speed bar is only shown when ownship's absolute speed along that axis is above a specified breakout speed. This declutters the display for near-zero speeds, and serves to sensitize the pilot to non-zero speeds. The digital readout of each axis' speed has a colored background that changes from green to red when the speed approaches an operating limit. Magenta pointers lying along the peripheral Altitude, Distance, and Cross-Distance axes indicate the separation remaining between ownship and the landing zone. If the approach was curved in the horizontal plane, Distance would represent distance along the curved trajectory, and Cross-Distance the horizontal separation normal to the trajectory's tangent.

Fig. 7 shows a progression sequence from maneuver entry through touchdown. An autopilot was used to track the guidance to provide an illustration of perfect tracking. In this example, predicted position was projected in time using both instantaneous velocity and acceleration, (hence the magenta prediction segments exhibit curvature). Descent commences after clearing a 100 foot high obstacle, at which point the helicopter speed is 10 knots and the distance to landing 290 feet. Since the approach is a straight-in, the lateral guidance is a vertical line originating from the display's center. After clearing the obstacle, Fig. 7b shows a sink rate of 395 feet/minute and a forward speed of 10 knots. In Fig. 7e a horizontal line on the right representing the landing target has come into view from above, and a horizontal line on the left representing the ground plane has come into view from below. At touchdown in Fig. 7f the target sink rate was 120 feet/min, and the target forward speed was zero knots.

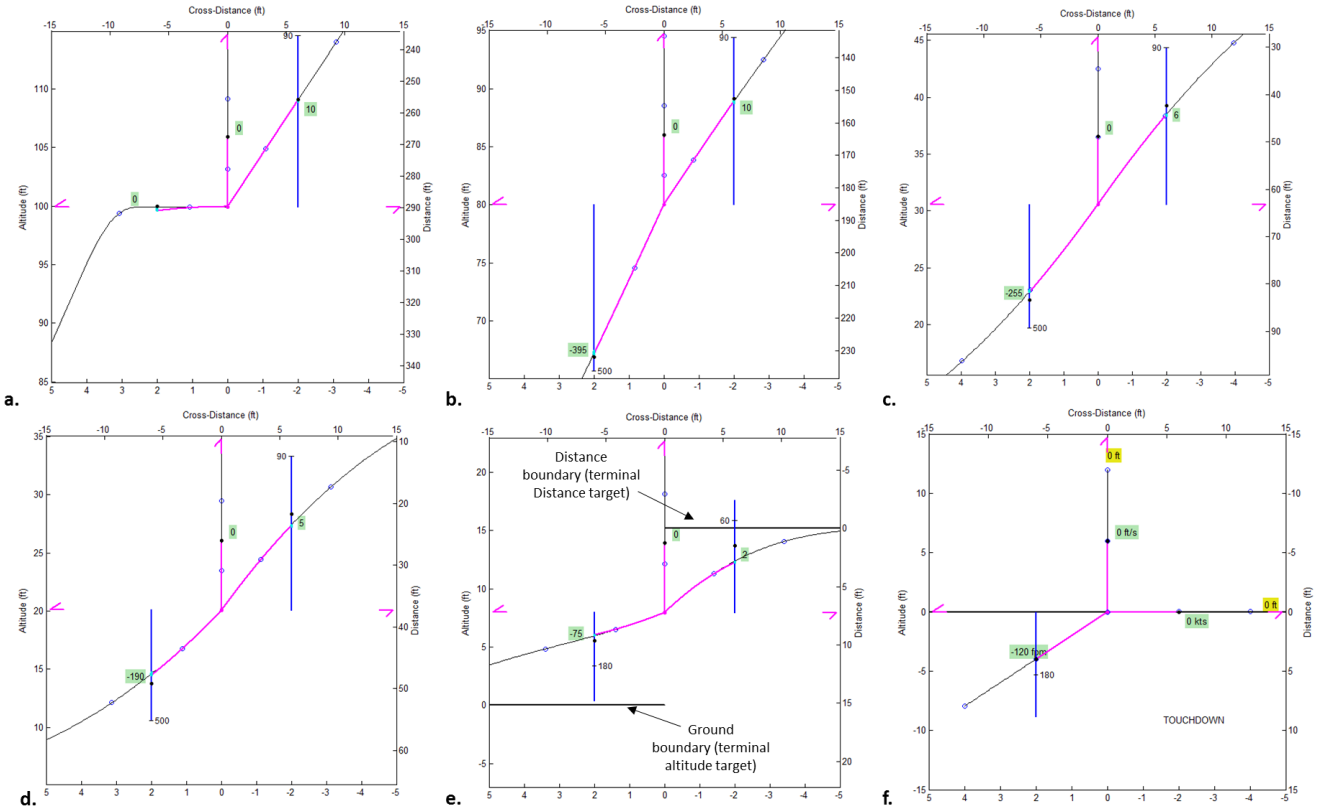

Fig. 7. : Obstacle-clearance landing sequence.

2.3 Predictor Design Considerations

A predictor can introduce large magnitude and/or high frequency response to disturbance, depending on the predictor design and the disturbance spectrum. Significantly, much of the research with 3D predictive visual displays has focused on disturbance-free performance. A notable exception presented by Mulder [9], which investigated the effect of turbulence while using a flight path vector (FPV) for tunnel-in-the-sky flight. The FPV is used by the pilot as a predictor of aircraft motion. In particular, Mulder reports “a pilot’s use of the FPV is significantly degraded when the bandwidth of the turbulence acting on the vehicle increases. In the high gust conditions, the pilot could have performed even better *without* the FPV.”

Another potential challenge with predictors is that vehicle modes that degrade handling qualities (such as lightly-damped modes during helicopter sling-load operation) can be excited by disturbances when employing prediction. Other troublesome vehicle dynamics, such as non-minimum phase zeros, can also make prediction compensation in the vicinity of crossover (via inverting vehicle dynamics and inserting an integrator) challenging. Furthermore, cancellation of lightly-damped modes is a poor design approach since the exact composition of a mode is unknown and can change over time. The predictor-vehicle suite ($H_{PR}G_c$) that the pilot must invert for feedforward control may thus be far more complex than the ideal *K/s* integrator, significantly diminishing the information value of preview and placing a greater burden on pilot compensatory control G_c. In other words, the further ($H_{PR}G_c$) departs from *K/s*, the more difficult for the pilot to generate the equalization that satisfies the Crossover Model [7] paradigm. An additional requirement is that the temporal meaning of the predictor’s output is preserved.

Kinematic prediction is employed by AGVA in the example presented herein, where the aircraft position is projected T_{PR} seconds out based on the weighted instantaneous position derivatives

velocity, acceleration, and jerk. As an example, kinematic prediction is applied to dynamics that are similar to the longitudinal position response of the H-60 Black Hawk to cyclic input during hover. Fig. 8 shows the approximate transfer function, (Eqn. 5) and its associated bode plot. Beyond 0.4 rad/sec the pilot is required to close the velocity and acceleration inner-loops for stable outer-loop control of position (this is what is done with the Apache hover symbology, which provides velocity and acceleration cueing). Rather than having the pilot close inner loops, a predictor can be employed to effectively close those loops and present the pilot with a single target to track. Eqn. 6 gives the predictor's position projection based on the three derivatives, and Eqn. 7 is its transfer function. Through proper selection of T_{PR} and weightings on the derivatives, the bode plot of the vehicle-predictor ($H_{PR}G_c$) combination can be shaped such that the frequency response is essentially flat beyond 1 rad/sec. To employ feedforward information such as previewed guidance the pilot would invert ($H_{PR}G_c$) as indicated in Eqn. 2, provided the aircraft motion arises predominantly from pilot control inputs compared to motion due to gust.

When gust effects are significant (i.e. during shipboard hover), compensatory control shares prominence with feedforward control, so that ($H_{PR}G_c$) should resemble an integrator as was given in Eqn. 3. In Fig. 9 this is accomplished using velocity and acceleration, and a time projection that is different from the one used in Fig. 8. When the pilot inverts this (Eqn. 4) to make use of feedforward information, more effort is required than when feedforward was used (see Fig. 8) (pure lead compensation is more difficult than operating as a pure gain), but this is the price of having to conduct compensatory control at the same time. If the predictor of Fig. 8 using jerk, acceleration and velocity were employed with compensatory control (i.e. disturbance is significant), the pilot would be forced to operate at a frequency well above or below 1 rad/sec since the vehicle dynamics undergo rapid change in the region of 1 rad/s (pilots cannot provide effective compensation when operating in such regions [Ref. 7].

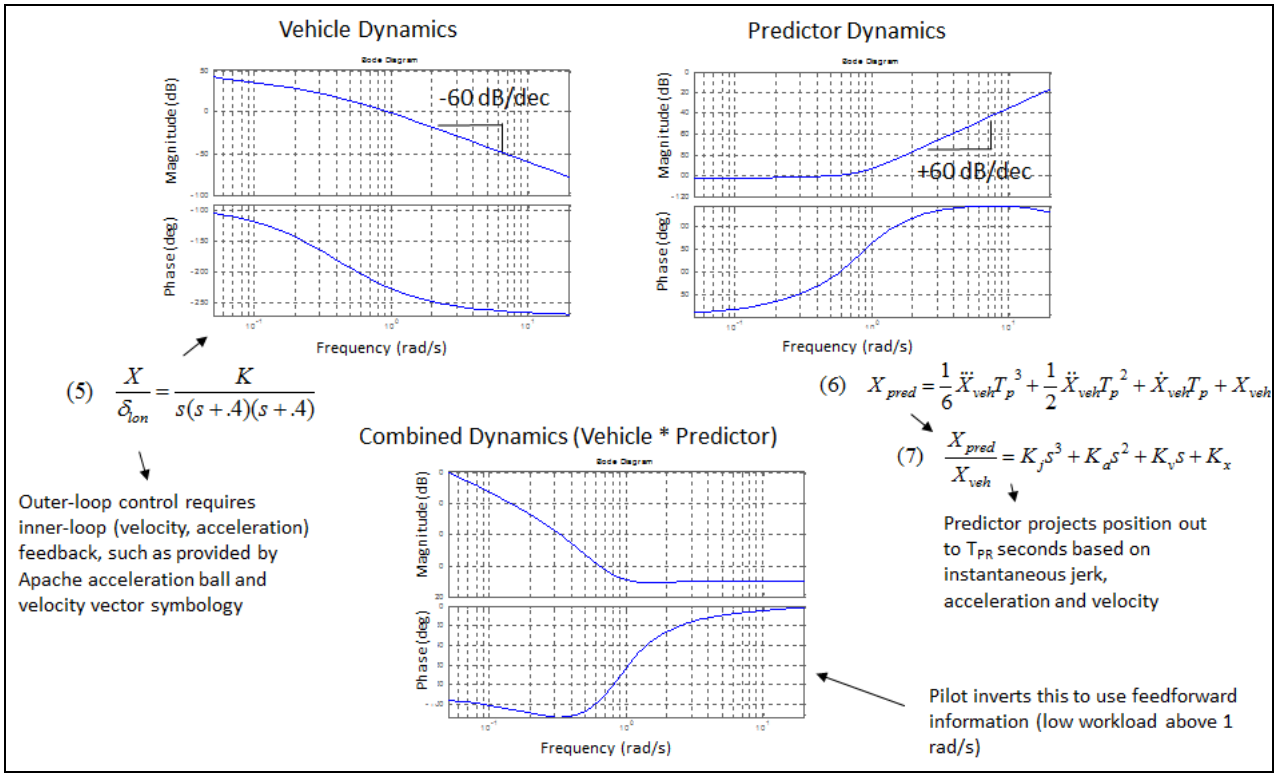

Fig. 8. Predictor design for UH-60 longitudinal hover dynamics when gust disturbance is negligible.

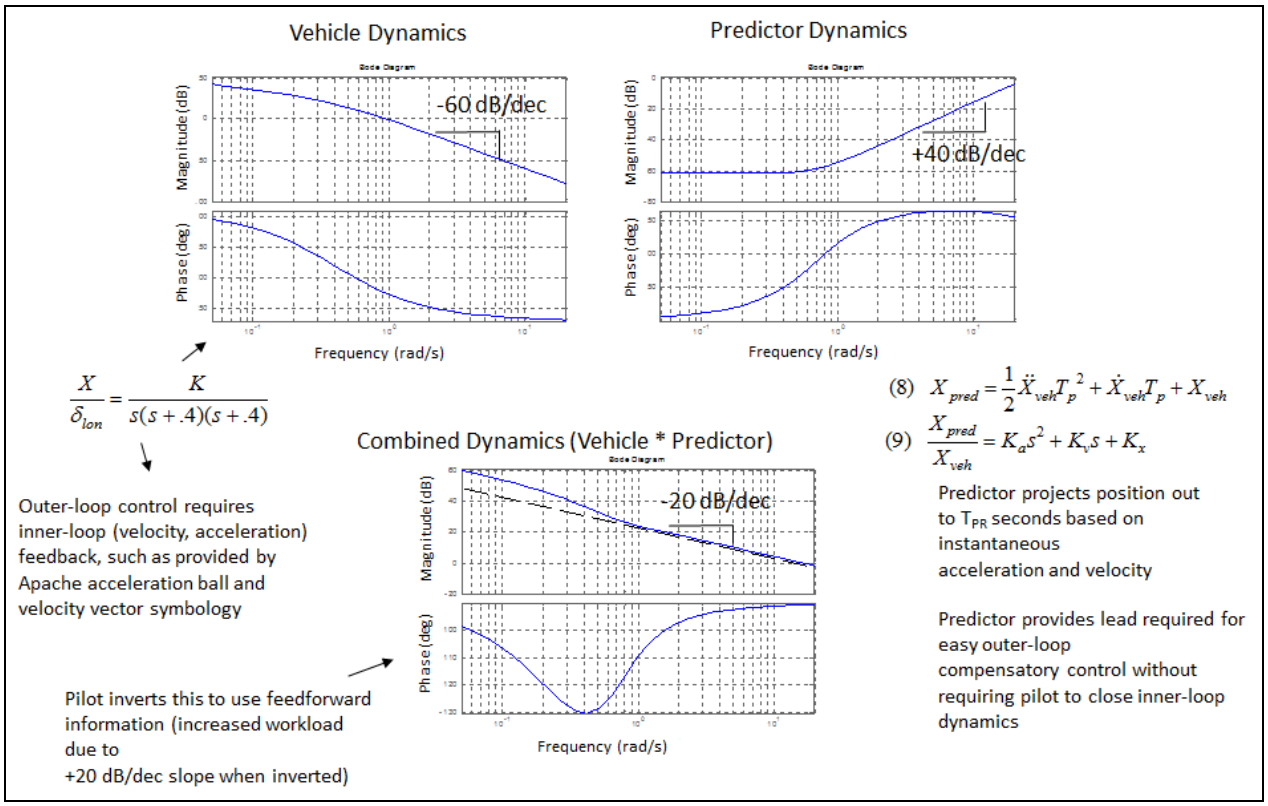

Fig. 9. Predictor design for UH-60 longitudinal hover dynamics when gust disturbance is significant.

3 EXPERIMENTAL PROTOCOL AND RESULTS

3.1 Protocol

Four male subjects took part in the study. Three were Experimental Test Pilots (graduates of Navy Test Pilot School) with 1,900, 1,900, and 2,450 rotary wing flight hours. The fourth subject had logged 800 hours of rotary wing flight time. Three prediction display configurations were tested with each subject (repeated-measures design): Jerk (incorporating jerk, acceleration, and velocity derivatives); Acceleration (incorporating acceleration and velocity derivatives); and Velocity (incorporating only velocity for prediction). The landing maneuver profile that was flown with all display configurations is shown in Fig. 10 (approach was a straight-in). The approach began at a height of 100 feet, 10 knots forward speed, zero sink rate, and 250 feet from the landing zone. The approach guidance terminated after 27 seconds with zero forward/lateral speed and a vertical sink rate of 120 feet/minute. Pilots flew the profile using the AGVA display and a gamepad as the input device: left knob (fore/aft) was used as collective, right knob (fore/aft) was longitudinal cyclic, and right knob (left/right) was lateral cyclic. AGVA was displayed on a 1280x800 resolution, 15.6" monitor. Each of the simulated vehicle's three axes of translation were given the same dynamics so that vehicle response would not be a contributing factor for differences in tracking performance between axes. The dynamics used for each axis approximate the longitudinal position response of the H-60 Black Hawk to cyclic input during hover, and the dynamics between axes were uncoupled.

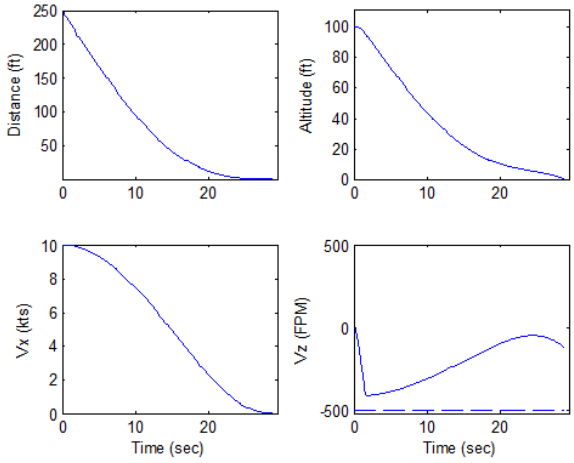

Fig. 10. Rapid-deceleration landing profile.

Subjects were allowed to practice flying each predictor type until they felt comfortable with its dynamics. Subjects requested at most two practice runs for each predictor. The order of predictor flown by each subject is shown in Table 1. J denotes the Jerk predictor, A denotes Acceleration predictor, and V denotes Velocity predictor. For instance, subject A flew the Jerk predictor three times, followed by the Acceleration predictor three times, etc.

Table 1 Test Matrix of Predictor Order

Subject						
A	JJJ	AAA	VVV	JJJ	AAA	VVV
B	AAA	VVV	JJJ	AAA	VVV	JJJ
C	VVV	AAA	JJJ	VVV	AAA	JJJ
D	JJJ	VVV	AAA	JJJ	AAA	VVV

3.2 Results

Fig. 11 compares one subject's vehicle response time traces with the prescribed guidance for the three predictor schemes. Visual inspection of range, altitude and cross-range indicates position tracking was roughly the same for all three predictor types, whereas the position rates were markedly different. Velocity prediction appeared to produce pronounced oscillations in forward speed and sink rate, Acceleration prediction less so, and Jerk prediction did not seem to induce oscillations in any axis.

Average touchdown error was compared across predictors in Fig. 12. In general Acceleration prediction yields considerably less error and variation than Velocity, with Jerk appearing to have slightly less error and variation than Acceleration. However, the accuracy and precision for the poorest performer, Velocity prediction, is excellent. In Fig. 13 the pilot input control rates (over the course of the entire maneuver) are normalized to the Velocity prediction rates. Consistent with the position rate activity seen in Fig. 12 for one subject, the overall control rate activity for all pilots substantially diminishes going from Acceleration to Velocity, and again going from Acceleration to Jerk. Finally, subjective ratings of pilot spare capacity using the Bedford scale [Ref.10] were compared. The Bedford scale ranges from 1 to 10, where 10 denotes task abandonment due to excessive effort, and 1 denotes the task insignificantly affected spare capacity. In Fig. 14a the absolute ratings decrease (i.e. spare capacity increases) comparing Acceleration to Velocity, and Jerk to Acceleration prediction. In Fig. 14b the change in rating relative to Velocity rating averaged -2 for Acceleration, and -3.5 for Jerk.

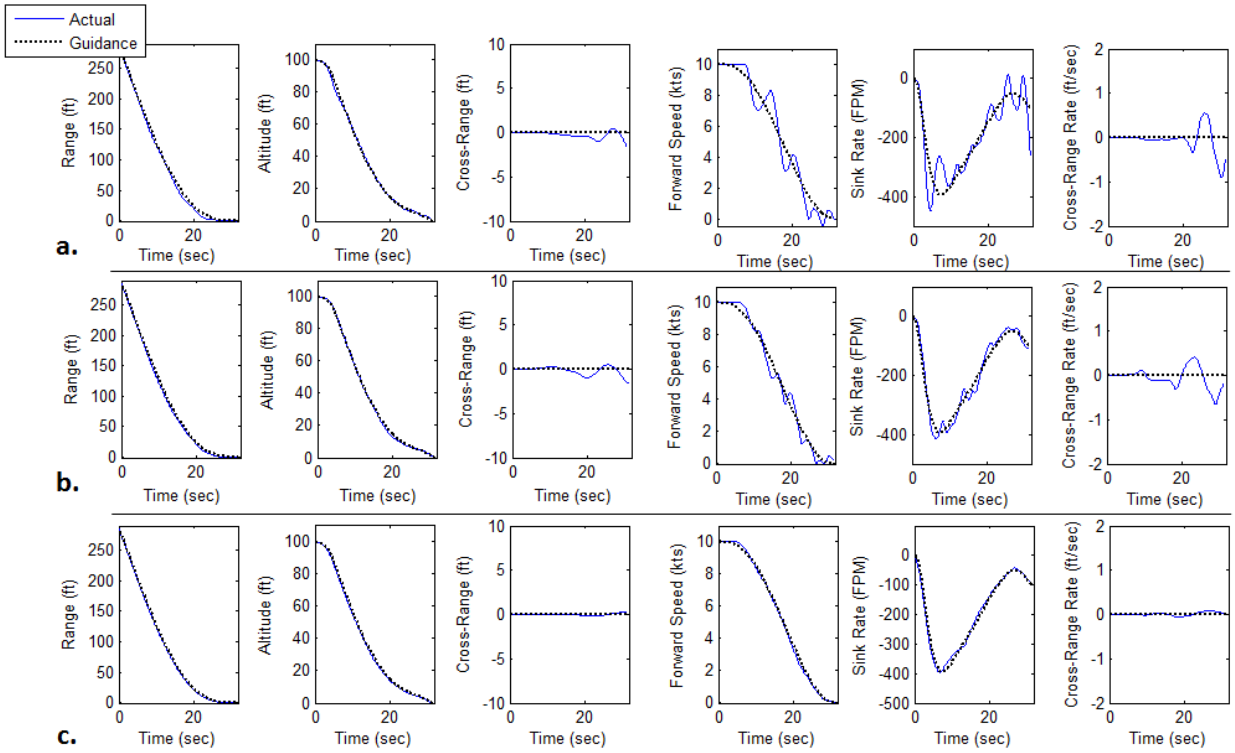

Fig. 11. Vehicle response time traces (solid blue) superimposed on guidance (dotted black) using three predictor schemes: a) Velocity; b) Acceleration; c) Jerk.

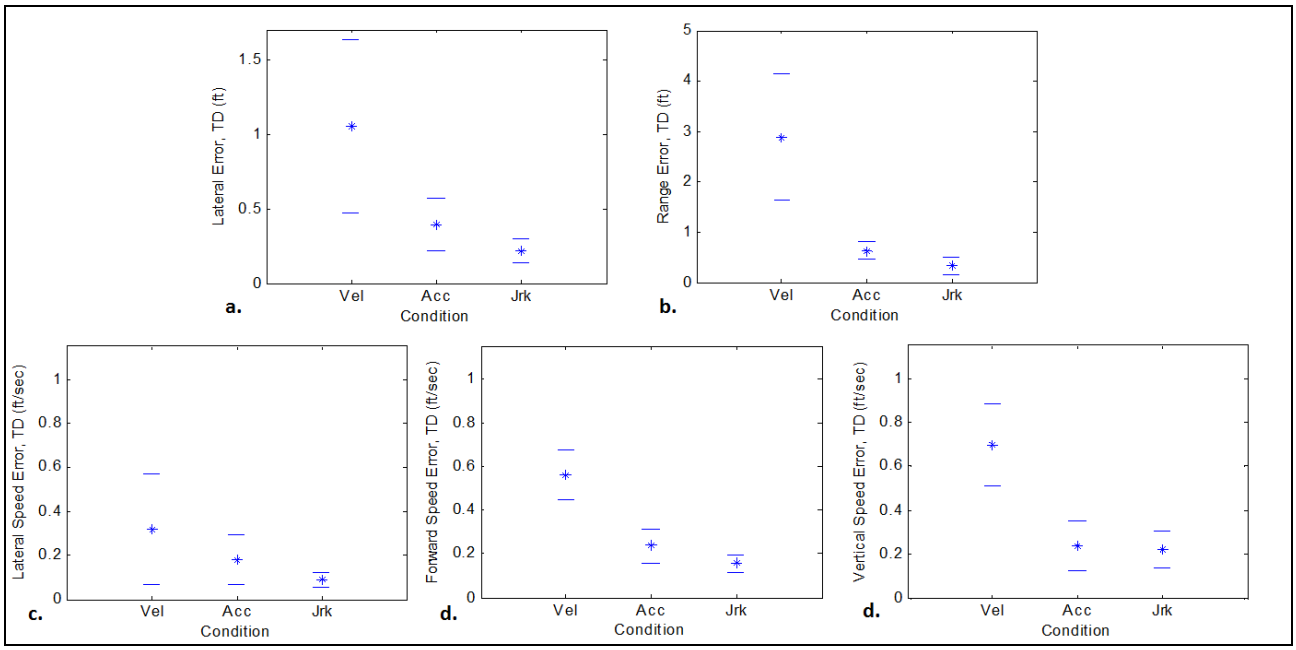

Fig. 12. Touchdown error comparisons between predictor schemes: a) Lateral position; b) Range position; c) Lateral speed; d) Forward speed; e) Vertical speed (standard deviation bars bracket the means).

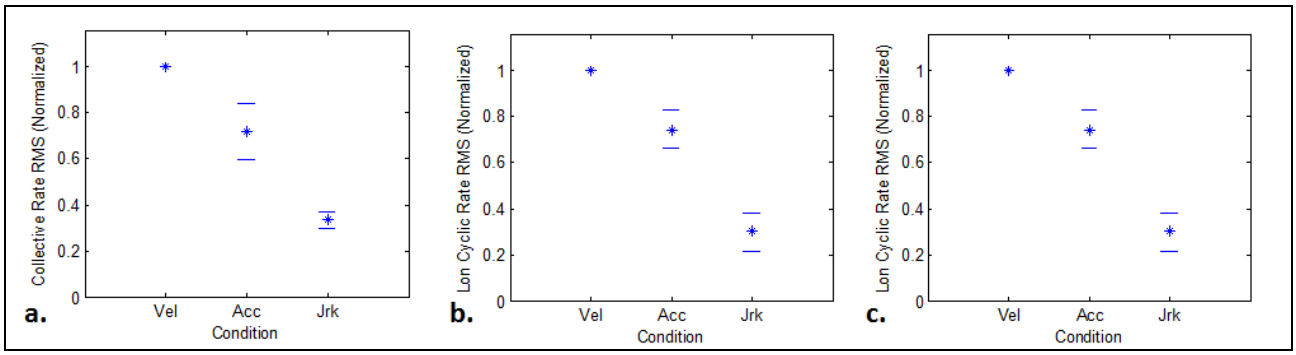

Fig. 13. Pilot control rates (normalized) comparisons between predictor schemes: a) Collective; b) Longitudinal; c) Lateral (standard deviation bars bracket the means).

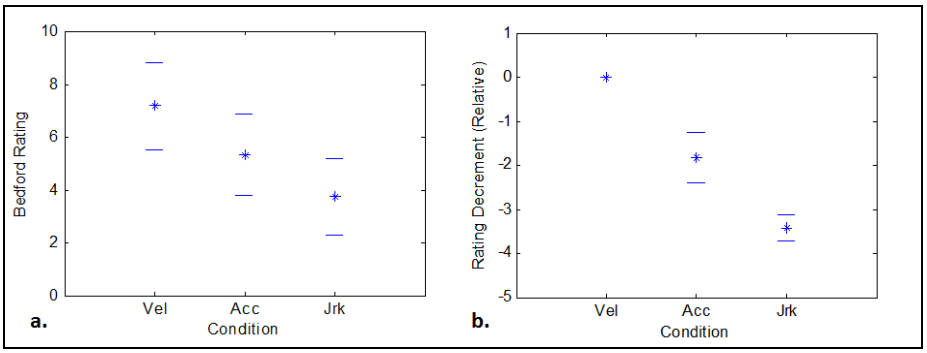

Fig. 14. Bedford rating [Ref. 10] comparisons between predictor types: a) Absolute; b) Differential (standard deviation bars bracket the means).

4 DISCUSSION

The approach profile commanded by the guidance used in this experiment was based on actual UH-60 data collected at Moffett Field during an aggressive obstacle-clearance maneuver (flown in unrestricted visibility using out-the-window pilotage). The following factors would have made the simulated approach and landing task more challenging than what the data-collection pilot flew: 1) Absence of key visual cues that are used during out-the window flight, such as motion parallax, relative size, relative density, occlusion, height in visual field [Ref.11]; 2) Simulated vehicle response in the vertical axis was acceleration-command (same as the other two axes, longitudinal and lateral), whereas in the actual aircraft the vertical response is rate-command, which is easier to fly [Ref. 12]; 3) Lack of vestibular feedback in the fixed-base simulation, which would increase pilot latency [Ref. 7].

The four pilots quickly adapted to the non-conventional AGVA display format. At most two practice approaches per prediction type were needed for each pilot to declare they were comfortable with the display. Since each run lasted approximately 30 seconds, the maximum total practice time each pilot required was less than 3 minutes.

Although the sample size of this preliminary experiment was very small, the initial results indicate that predictor dynamics play a critical role in system performance and pilot workload. The most experienced test pilot remarked it was difficult to believe he was flying the same aircraft when using the different predictor types. Touchdown accuracy and precision for the poorest performer, Velocity prediction, was comparable to performance observed for out-the-window landings. The use of Jerk prediction with AGVA yielded very accurate and consistent results.

The theoretical development addressing predictor effects on pilot workload and performance appeared to be supported by the preliminary results – as predictor compensation progressed from Velocity to Jerk, the pilot compensation had been anticipated to become easier and system stability to improve.

Gust disturbance was not employed in this experiment as the main objectives were to investigate the efficacy of AGVA's display format and the effects of predictor design using previewed guidance. As noted earlier in the section "Predictor Design Considerations", when disturbance is significant it should be factored into predictor dynamics in order to balance the pilot's compensatory and feedforward tracking paths. One approach for accounting for gust was proposed in Fig. 9, which was the design behind the Acceleration predictor. While the Jerk predictor produced the best performance and subjective ratings, the Acceleration design yielded performance that was not substantially different, and subjective ratings slightly less favorable. However, in the presence of significant disturbance (i.e. aircraft motion due to gust is comparable to the motion induced by pilot commands), the Acceleration predictor would be far easier to control than Jerk - Jerk would amplify the gust's higher frequency spectrum, and the pilot would be forced to operate at a low crossover frequency to avoid being over-driven, which would degrade performance.

5 CONCLUSIONS

A novel space-time format was proposed for displaying: 1) Previewed 4D guidance information; 2) Projected (predicted) state relative to the guidance preview; and 3) Current state relative to current guidance and terminal objectives. A key objective of the display was to allow the pilot to perceive and control each axis of translation as part of an integrated pattern, thus distributing attention equitably. The preliminary test results appear to support the theoretical development that addressed predictor effects on pilot workload and performance. Pilots rapidly adapted to AGVA's non-conventional format, and demonstrated high precision and accuracy when flying an aggressive approach-to-land maneuver. Future testing with AGVA will be conducted with gust disturbance, as well as in a high-fidelity UH-60 simulator.

Acknowledgments
This work was supported by cooperative agreement NNX13AI30A between the U.S. Army Aviation Development Directorate and San Jose State University. This paper has been approved for public release: unlimited distribution.

REFERENCES

1. Padfield, G.: The Tau of Flight Control. In: Royal Aeronautical Society, Volume: 115, Number: 1171. (2011)
2. Bachelder, E.: Perception-Based Synthetic Cueing for Night Vision Device Hover Operations, MIT Ph.D. Dissertation. (2000)
3. Mulder, M.: Cybernetics of Tunnel-in-the-Sky Displays. Ph.D. Dissertation, Faculty of Aerospace Engineering, Delft University of Technology (ISBN 90-407-1963-2). (1999)
4. Boeing, http://www.boeing.com/commercial/aeromagazine/articles/2012_q1/3/
5. Sachs, G., Sperl, R., Sturhan, I.: Curved and Steep Approach Flight Tests of a Low Cost 3D Display for General Aviation Aircraft. ICAS Congress. (2006)
6. Arents, R., Groeneweg, J., Borst, C., van Paassen, M., Mulder, M.:,Predictive Landing Guidance in Synthetic Vision Displays. In: The Open Aerospace Engineering Journal, 4, 11-25 11. (2011)
7. McRuer, D., Krendal, E.: Mathematical Models of Human Pilot Behavior. AGARD-AG-188. (1974)
8. Arents, R., Groeneweg, J., Borst, C., van Paassen, M., Mulder, M.:,Predictive Landing Guidance in Synthetic Vision Displays. In: The Open Aerospace Engineering Journal, 4, 11-25 11. (2011)
9. Mulder, M.: Flight-path Vector Symbology in Tunnel-in-the-sky Displays. In: Conference on human decision making and manual control, Loughborough, October 25-27. (1999)
10. Roscoe, A., Ellis, G.:A Subjective Rating Scale for Assessing Pilot Workload in Flight: A Decade of Practical Use, Royal Aerospace Establishment, Technical Report TR 90019, March 1990.
11. Cutting, J., Vishton, P.: Perceiving Layout and Knowing Distances: The Integration, Relative Potency, and Contextual Use of Different Information about Depth. In W. Epstein & S. Rogers (Eds), Handbook of Perception and Cognition. Vol. 5: Perception of Space and Motion, San Diego, CA, 1995.
12. ADS-33E-PRF Rotorcraft Handling Qualities Specification for U.S. Army Aeroflightdynamics Directorate, March 2000.